ITEC Asia-Pacific 2014 1569949765

A comparative study of equivalent circuit models and enhanced equivalent circuit models of lithium-ion batteries with different model structures

Guangming Liu [a], Languang Lu [a], Hong Fu [b], Jianfeng Hua [c],Jianqiu Li [a], Minggao Ouyang [a], Yanjing Wang [b], Shan Xue [b], Ping Chen [b],

[a] State Key Laboratory of Automotive Safety and Energy, Tsinghua University, Beijing 100084, P.R. China
[b] Chongqing Changan New Energy Automobile CO., Ltd, Chongqing 401120, P.R. China
[c] Key Power Technology Corporation, Ltd, Beijing 100084, P.R. China

e-mail: lgm06@mails.tsinghua.edu.cn

***Abstract*—Lithium-ion battery model is critical for voltage and state of charge (SOC) determination, and the equivalent circuit model (ECM) is frequently implemented in real-time cases due to low complexity, but the low-SOC-area performance requires improvement. This paper introduces an enhanced equivalent circuit model (EECM) based on electrochemical analysis, in which the surface SOC (SOC_{surf}) reflects the lithium concentration at the particle surface and is used to determine the terminal voltage. Five empirical based models with different model structures (in which two ECMs and three EECMs included) are selected to compare the model accuracy and complexity. Experiments were carried out on a battery test system with a temperature chamber, and a modified hybrid pulse power characterization (HPPC) profile was employed to measure the battery dynamic response. The genetic algorithm method is implemented in model parameterization, and the voltage estimation accuracy of the five empirical models is compared in SOC range 0~100%. The results show that the EECMs considering SOC_{surf} provides better accuracy than the traditional ECMs in low-SOC area, and the EECM with one RC component and one DS component provides the optimum performance considering accuracy and complexity.**

Keywords—lithium-ion battery; equivalent circuit model; surface state of charge; model comparison; low state-of-charge area

I. INTRODUCTION

Electric vehicles (EVs), i.e. hybrid electric vehicles (HEVs), plug-in hybrid electric vehicles, and pure electric vehicles (PEVs) have attracted a lot of attention owing to the significant performance improvement in environmental friendliness and driving economy compared with the traditional vehicles. PEVs are capable of zero-emission driving and hence are the focus of the present research for urban driving cases. However, the driving range of PEV is not competitive and is hence the main barrier from the consumers' viewpoint [1], since the battery pack as the only onboard energy storage system is with limited energy density. In order to limit the passengers' anxiety about an unreachable destination due to inaccurate prediction of PEV remaining driving range (RDR), the battery remaining discharge energy (E_{RDE}) needs to be precisely estimated [2]. The determination of E_{RDE} relies on an accurate battery model to calculate the terminal voltage (U_t) and the state of charge (SOC). Plenty of battery models were developed and discussed, in which the equivalent circuit model (ECM) is frequently implemented in real-time applications due to its simplicity. However, since the Li-ion battery shows strong nonlinearity in low-SOC area, the SOC and voltage calculation results from the ECM are not satisfying, and could lead to obvious error in RDR prediction and hence the passengers' range anxiety. If the battery model performance in low-SOC area is raised, the E_{RDE} estimation accuracy could hence be improved to obtain a better RDR result.

Most of the studies on lithium-ion battery modeling focus on equivalent circuit models (ECM) [3-8] and electrochemical models [9-12]. The ECM employs basic electric components to reflect the terminal voltage output under a current profile, and is frequently performed in real-time cases for its simplicity. However, the structure of ECM is usually empirical based and could not reflect the electrochemical process during charge and discharge well. The electrochemistry-based battery model is another focus of the current studies, in which terminal voltage and SOC are calculated according to the electrochemical reaction process. Based on the porous electrode structure, the electrochemical model analyzes the concentration distribution as well as the potential differences in sold phase and electrolyte phase [9], and comes out with the potential difference in the positive and negative current collectors to represent the terminal voltage. Electrochemical model deals with more information than the ECM and is potential to provide more accurate results, but the high computational complexity makes the electrochemistry-based models not suitable for online implementations, and the multiple electrochemical parameters could not be easily determined by automotive manufacturers.

This paper tries to present an improved empirical battery model based on the electrochemical process. The so-called enhanced equivalent circuit model (EECM) represents the lithium concentration at the electrode particle surface by the

term surface SOC (SOC_{surf}) to describe the solid-phase diffusion during discharging and charging. The EECMs and the ECMs with different structures are compared to verify the advantage of EECM in voltage estimation accuracy, and to find an optimum model structure considering the precision as well as the computational accuracy. The remainder of this paper is as follows. Section 2 introduces the enhanced equivalent circuit battery model based on the simplified electrochemical model, and lists the five potential model structures for performance comparison. Section 3 explains the experimental setup. The parameterization process as well as the comparison of the five empirical based models is discussed in detail in Section 4, and Section 5 is the conclusion.

II. MODELING

A. Discussion and modification of battery ECM based on electrochemical model

This research aims to evaluate the real-time-applicable battery empirical models, and the single-particle electrochemical model (SPM) is used as the theoretical basis in our discussion [11,12]. In SPM, the dynamics of the electrode particles as well as the current density are seen as identical within an electrode, and the negative and positive electrodes could be seen as two electrode particles. Simplified from the two-dimensional electrochemical model, Fig. 1 discusses the discharge process in SPM framework. Lithium de-intercalates from the anode particle, flows in electrolyte, and intercalates into the cathode particle. There exist two solid-phase diffusion processes within the negative and positive electrode particles, the double-layer-caused potential drop at the anode and cathode reaction interfaces, the liquid-phase potential drop within the electrolyte, and other voltage drops causes by the solid-electrolyte-interface (SEI) film and the current collector resistance, etc. The solid-phase diffusion processes result in the battery equilibrium potential U_{equ} through the lithium concentration at the surface of negative and positive electrode particles ($c_{surf,p}$ and $c_{surf,n}$), which is combined with the dynamic potential distributions within the battery to decide the terminal voltage, as in Eq. (1). Here U_0 represents the direct voltage drop by the liquid-phase potential distribution and the SEI film, and $U_{DL,n}$ and $U_{DL,p}$ are the voltage drops resulting from the double layer effect in the charge transfer process.

$$U_t = U_{equ}(c_{surf,p}, c_{surf,n}) - U_0 - U_{DL,n} - U_{DL,p} \tag{1}$$

In electrochemical model, SOC is reflected by the average lithium concentration in electrode particle (c_{avg}). The present SOC could be calculated by the anode average concentration $c_{avg,n}$ or the $c_{avg,p}$ for the cathode as in Eq. (2).

$$\mathrm{SOC} = \frac{c_{avg,n} - c_{avg,n,0\%}}{c_{avg,n,100\%} - c_{avg,n,0\%}} = \frac{c_{avg,p} - c_{avg,p,0\%}}{c_{avg,p,100\%} - c_{avg,p,0\%}} \tag{2}$$

Since the terminal voltage U_t is straightly related to the lithium concentration at the surface rather than the average concentration c_{avg}, the term SOC does not match the purpose of the battery voltage model perfectly. But as a simplified empirical model, the ECM uses the average SOC to determine the open circuit voltage (OCV) and the voltage output, in which SOC is calculated by current integration. The normally implemented ECM consists of a pure resistor Ro and n groups of RC components (i.e. resistor-capacitor parallel circuits), as in Fig. 2. The ECM-calculated terminal voltage is represented in Eq. (3), in which $U_{p,i}$ is the polarization voltage of the i-th RC component.

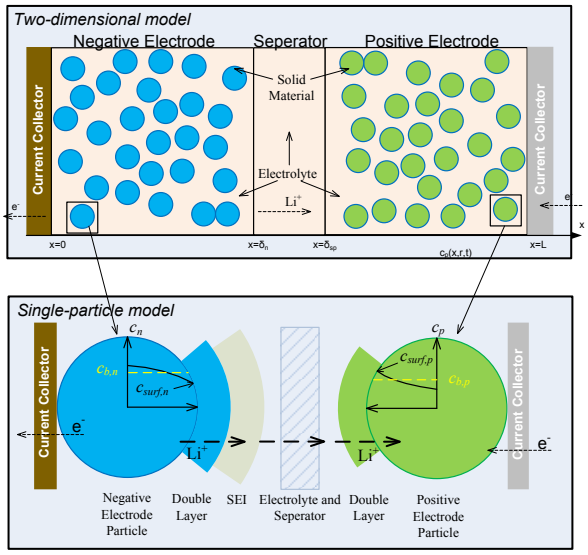

Fig. 1. Explanation of lithium-ion battery discharge process based on single-particle model

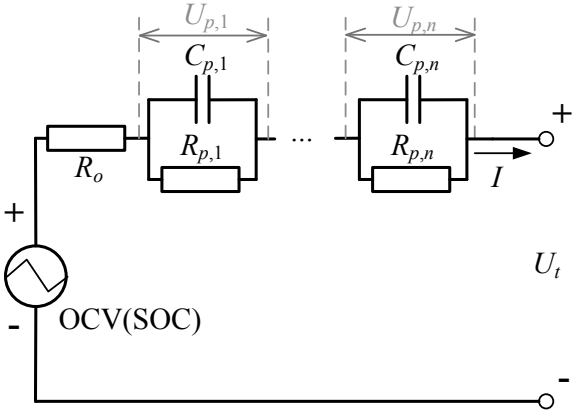

Fig. 2. Schematic of battery equivalent circuit model (ECM) with n groups of RC components

$$U_t = \mathrm{OCV(SOC)} - I \cdot R_o - U_{p,1} - \ldots - U_{p,n} \tag{3}$$

It is clear that the ECM implements the average SOC and could hence not reflect the equilibrium potential U_{equ} i.e. the particle surface concentration directly. The difference between surface and average concentration could only be approximately represented by the polarization voltage $U_{p,i}$. The equilibrium potential U_{equ} shows very strong nonlinearity with the lithium concentration as demonstrated in Fig. 3, in which the abscissa SOC is proportionally related to the lithium concentration. When the curve is relatively flat, i.e. at the high and middle SOC range, the difference between average and surface

concentration results in little voltage change (OCV_{high} versus $U_{equ,high}$), and the ECM could estimate the voltage very well. However, the U_{equ} curve becomes much steeper at low-SOC range, and the concentration difference would lead to a relatively large potential difference (OCV_{low} versus $U_{equ,low}$), which weakens the performance of ECM.

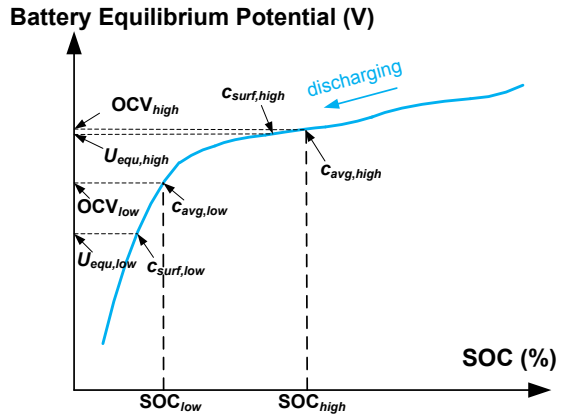

Fig. 3. Illustration of surface and average lithium concentration and its influence on voltage determination in ECM

In order to improve the ECM accuracy, the term surface SOC (SOC_{surf}) is introduced to reflect the particle surface lithium concentration c_{surf}, as in Eq. (4). Since the separate calibration of anode and cathode properties is relatively inconvenient in real-world applications, a single SOC_{surf} is used to approximate the subtraction of two electrodes. The difference of c_{surf} and c_{avg} in solid-phase diffusion process could be expressed as the sum of two one-state processes indicating the solid-phase diffusion [13], as in Eq. (5), in which $I_{F,1}$ and $I_{F,2}$ are the faradic currents in the electrodes. The relationship of SOC_{surf} and SOC is hence written as Eq. (6).

$$SOC_{surf,n} = c_{surf} / c_{avg} \cdot SOC \tag{4}$$

$$\Delta c = k_{c,1} I_{F,1} \cdot (1 - e^{-t/\tau_{SD,1}}) + k_{c,2} I_{F,2} \cdot (1 - e^{-t/\tau_{SD,2}}) \tag{5}$$

$$\Delta SOC = k_{SD,1} I_{F,1} \cdot (1 - e^{-t/\tau_{SD,1}}) + k_{SD,2} I_{F,2} \cdot (1 - e^{-t/\tau_{SD,2}}) \tag{6}$$

Consequently, the ECM could be modified by implementing SOC_{surf} rather than SOC to reflect the real-time particle surface concentration. The enhanced equivalent circuit model (EECM) is hence introduced with the structure shown in Fig. 4. A new type of component (DS component) is added into the traditional ECM to calculate the difference between SOC and surface SOC, i.e. ΔSOC, and the OCV value is decided by SOC_{surf} rather than the average SOC. The DS component indicates a first-order process, but the output is a SOC value (which is named as ΔSOC_j for the j-th DS component) instead of the voltage drop as for the RC component. The input of the DS component is the faradic current which goes through the polarization resistor of the corresponded RC component. The voltage U_t in EECM is expressed in Eq. (7), and the SOC_{surf} is decided from the average SOC in Eq. (8).

$$U_t = OCV(SOC_{surf}) - I \cdot R_o - U_{p,1} - ... - U_{p,n} \tag{7}$$

$$SOC_{surf} = SOC - \Delta SOC_1 - ... - \Delta SOC_m \tag{8}$$

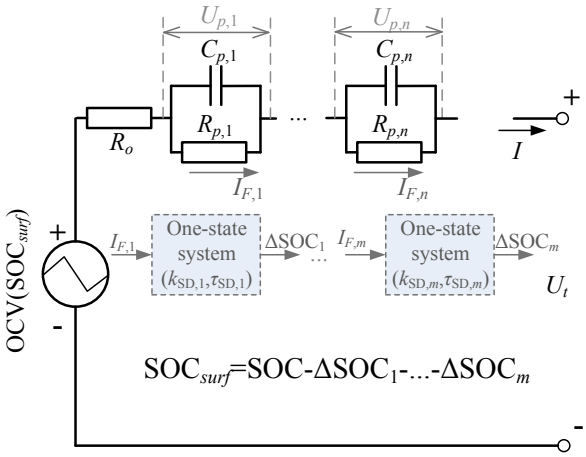

Fig. 4. Schematic of battery enhanced equivalent circuit model (EECM) with n groups of RC components and m groups of DS components

B. Comparison of models with different structures

As a result, the general EECM is equipped with n RC components and m DS components, in which m is equal to or smaller than n. The traditional ECM is in fact the EECM with m equaling 0. With the increase of component number, the voltage and SOC estimation accuracy could be generally improved at the cost of larger calculation amount. In order to find an optimum model structure with balanced accuracy and complexity, different model structures need to be compared. In this paper, we mainly check the relatively simple models, and the models with m larger than 2 are not discussed. Five equivalent circuit models are compared with the numbers of RC components (n) and DS components (m) listed in Table I with the names Model 1 to Model 5, and the to-be-determined states are also listed.

TABLE I. LIST OF FIVE EMPIRICAL BASED MODELS WITH DIFFERENT STRUCTURES

No.	Number of RC components (n)	Number of DS components (m)	States to be determined	Number of parameters to be determined
1	1	0	$U_{p,1}$	4
2	2	0	$U_{p,1}$, $U_{p,2}$	6
3	1	1	$U_{p,1}$, ΔSOC_1	6
4	2	1	$U_{p,1}$, $U_{p,2}$, ΔSOC_1	8
5	2	2	$U_{p,1}$, $U_{p,2}$, ΔSOC_1, ΔSOC_2	10

Each state ($U_{p,i}$ or ΔSOC_j) requires two parameters (proportional factor and time constant), and the parameter numbers to be identified is listed, note that the ohmic resistance values in discharging and charging process are separately determined. It is noticed that the number of DS component in Model 1 and 2 is 0, indicating the traditional ECM. The performance comparison of the ECMs and the EECMs could be illustrated by Model 1-2 versus Model3-5.

III. EXPERIMENTAL

A type of lithium nickel-cobalt-manganese oxide/graphite (NCM-G) battery with 20-Ah nominal capacity was tested in this research, with the basic parameters listed in Table II. A Neware BTS-3000 test bench (current range -100~100 A) and a DGBELL BE-HL-150M3 temperature chamber (temperature range -40~150 ℃) were implemented in the experimental process.

TABLE II. BASIC PARAMETERS OF TEST BATTERY

Parameter	Value
Material	$Li(Ni_xMn_yCo_{1-x-y})O_2$/Graphite
Nominal capacity (Ah)	20
Maximum discharge current (A)	4 C (80 A)
Maximum charge current (A)	1 C (20 A)
Allowed voltage range (V)	2.75~4.2
Allowed discharge temperature (℃)	-20~55
Allowed charge temperature (℃)	0~45

The hybrid pulse power characterization (HPPC) test was performed on the battery for parameter identification and model accuracy validation [14]. A slight modification was made on the original HPPC profile by lengthening the discharge period to 30 s to fit the PEV case, and the discharge period after the discharge and charge pulses was also used in parameter identification to keep the obtained parameters suitable for the constant-current discharge cases. As a result, four steps were included in the identification profile, i.e. the 30 s discharge pulse with 40 A (2 C) current, the 40 s pause between discharge and charge pulses, the 10 s charge pulse with 30 A (1.5 C) current, and the 280 s discharge period with nominal discharge rate 0.5 C (10 A). The duration 280 s for the constant-current discharge period is determined to move the battery SOC by 5%, hence the influence of SOC on battery parameters could be revealed. The test profile was followed by a 3-h rest to get rid of the polarization effect, and was performed from the fully-charged state until the discharge voltage limit. Twenty groups of test data were consequently obtained to analyze the battery property in different SOC range. The battery SOC-OCV relationship was determined as the mean value of low-rate discharging and charging voltage curves. Here 0.4-A current was implemented on the battery for discharging and charging, and the obtained OCV is shown in Fig. 5. It is noticed that the curve in high and middle SOC range is relatively flat and the period under 15% SOC shows obvious larger slope. This curve is later implemented in the five equivalent circuit models, in which the EECM (Models 3-5) uses SOC_{surf} to look up the equilibrium potential while the traditional ECM (Models 1-2) uses average SOC instead.

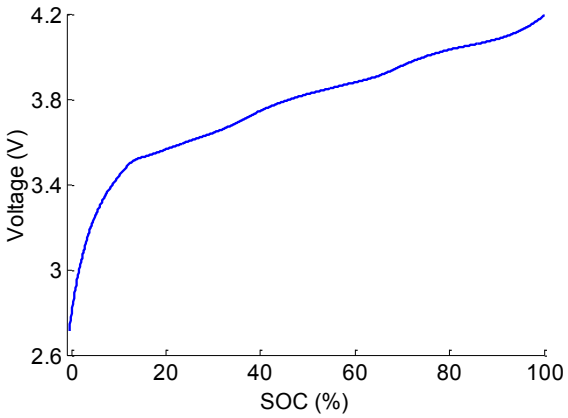

Fig. 5. Battery SOC-OCV relationship through 0.02 C discharge/charge data

IV. RESULTS

A. Parameter identification

Based on the experimental results, the parameterization process is executed on the five empirical models for comparison, as listed in Table 1. There exist a large number of parameters to be identified (four for Model 1, six for Model 2 and 3, eight for Model 4, and ten for Model 5), and an intelligent and stable identification method is needed for a reasonable parameter results. The genetic algorithm (GA) is hence a proper choice [15]. As a global optimization method, the GA could find the optimum for complex objective functions effectively, and is here carried out for the model parameter identification. The model voltage outputs follow Eq. (3) for the two ECMs and Eq. (7) for the three EECMs, and the root mean square error between voltage measurement and model-calculated voltage is determined as the cost function in GA optimization. The obtained parameters are implemented in Section 4.2 for model performance analysis.

B. Results analysis and comparison

Based on the experimental data, the model parameters are identified by the GA method according to five different model structures, and the difference between the measured voltage and the model-calculated voltage could be analyzed to reflect the model accuracy. The root mean square errors (RMSEs) of the calculated voltage from the to-be-compared models at different SOCs are shown in Fig. 6, in which the RMSEs of traditional ECMs (Models 1 and 2) are represented by blue markers while the RMSEs of EECMs (Models 3-5) are with red color. Note that each test point covers a 5%-SOC range, e.g., the point at 5% SOC reflects actually the model accuracy in the 0%~5% SOC range. The errors at middle and high SOC (SOC larger than 20%) SOCs are shown in Fig. 7, in which all the models illustrate good accuracy with RMSEs lower than 5 mV. It is noticed that the EECMs with red markers exhibit

slightly smaller error than the blue-colored ECMs. In the lower-than-20% SOC range, the difference among the models becomes much more obvious. The EECMs (Models 3-5) show clear advantages over the traditional ECMs (Models 1 and 2), indicating that the low-SOC-area voltage accuracy could be enhanced by the EECM with SOC_{surf} calculation. Taking the 5%-SOC case as an example, RMSE is reduced by more than 50% by employing any of the three EECMs. It is noticed that the increase of model parameters generally benefits the accuracy within the same model type (ECM or EECM), e.g. Model 2 versus Model 1, Model 5 versus Models 3 and 4. But the performance of the 2RC-1DS Model 4 and 1RC-1DS Model 3 is almost the same, implying that the low-SOC accuracy mainly depends on the number of DS components, and more RCs does little for the model performance.

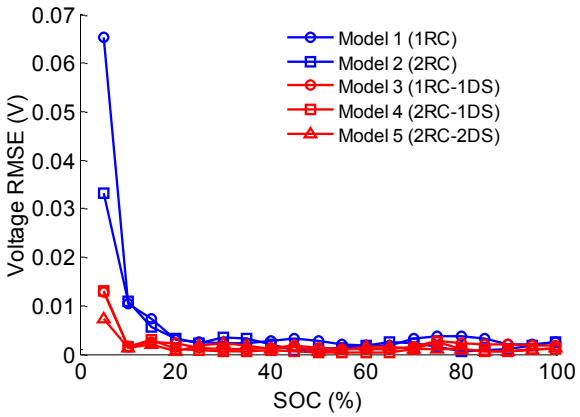

Fig. 6. Voltage RMSE comparison of five empirical models in the entire SOC range

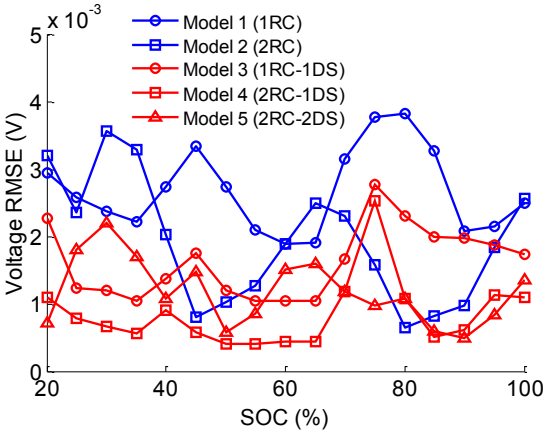

Fig. 7. Voltage RMSE comparison of five empirical models in SOC range 20%~100%

The model-calculated voltage is compared with the measurement result in Figs. 8-10. Three SOC points representing high-SOC area (80% SOC, in Fig. 8), middle-SOC area (40% SOC, in Fig. 9), and low-SOC area (5% SOC, in Fig. 10) are chosen to compare the accuracy of the empirical models. The red markers stand for the ECMs and the green ones are for the EECMs. At 80% SOC and 40% SOC, the voltage results from all the models correspond well with the experimental data, in which the green-colored EECMs illustrate slightly better result than the red-colored ECMs. At 5% SOC, all three EECM-determined voltage curves traces the measurement result tightly, which is more accurate than both of the ECMs (Models 1 and 2).

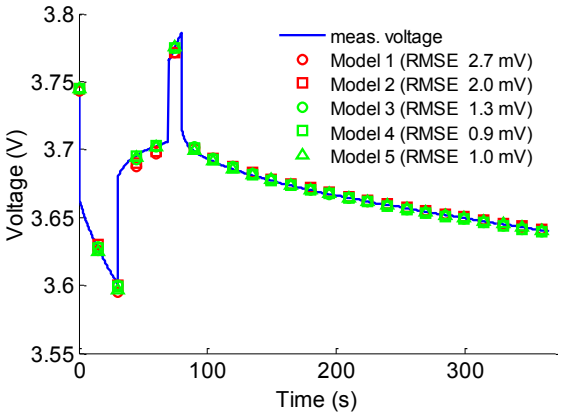

Fig. 8. Voltage estimation results of five empirical models at 80% SOC

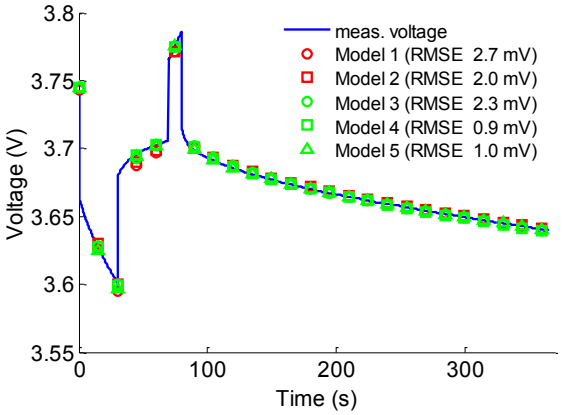

Fig. 9. Voltage estimation results of five empirical models at 40% SOC

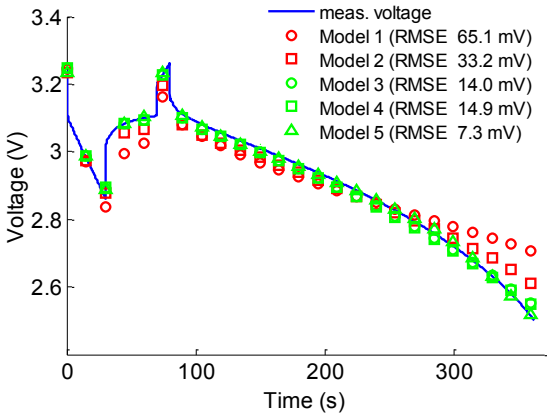

Fig. 10. Voltage estimation results of five empirical models at 5% SOC

From the above analysis, it is expressed that the EECMs with SOC_{surf} determination have a certain advantage over the ECM at low SOCs. And although Model 5 (2RC-2DS) presents the best accuracy, the model structure (with ten model parameters) is slightly more complicated than the six-parameter 1RC-1DS Model 3, which has the same complexity with the traditional 2RC ECM and could guarantee enough estimation accuracy in most cases with limited complexity. As a result, the 1RC-1DS EECM is proved as the proper model with balanced accuracy and complexity.

V. CONCLUSION

An onboard-applicable battery model is required to provide accurate terminal voltage and state of charge (SOC) results in the whole SOC range to precisely estimate battery remaining discharge energy (E_{RDE}) and remaining driving range (RDR) in electric vehicles. But the commonly-used equivalent circuit models (ECM) could not guarantee the low-SOC-range performance. In this paper, the enhanced equivalent circuit model (EECM) with improved accuracy in low-SOC area is introduced. Based on the traditional ECM, the EECM reflects the electrochemical solid-phase diffusion process by determining the particle surface SOC (SOC_{surf}), which is then employed to determine the terminal voltage. The EECM shows better performance in low-SOC range owing to the SOC_{surf} implementation rather than the average SOC for the ECM. The difference of SOC_{surf} and SOC (i.e. ΔSOC) is calculated by several one-state elements (DS components), and different numbers of RC elements and DS elements leads to the model performance difference considering accuracy and complexity. Three types of EECMs with different structures are compared with two traditional ECMs to validate the model improvement. The performance of the five empirical models is also evaluated to find the optimum model structure in onboard applications in view of accuracy and computing amount.

Under a modified HPPC profile, the NCM-G battery is tested and the parameters for the five models are separately determined through the genetic algorithm. Compared with the two ECMs, the voltage root mean square errors (RMSEs) in low-SOC area for the three EECMs are all reduced by more than 50%. And the 1RC-1DS EECM is proved as the proper model with balanced accuracy and complexity.

ACKNOWLEDGMENT

Support by the MOST (Ministry of Science and Technology) of China under the contracts of No. 2014DFG71590 and No. 2011AA11A227, and the MOE (Ministry of Education) of China under the contract of No. 2012DFA81190 is greatly acknowledged.

REFERENCES

[1] M.K. Hidrue, G.R. Parsons, W. Kempton, and M.P. Gardner, "Willingness to pay for electric vehicles and their attributes," Resour. Energ. Econ., vol. 33, pp. 686–705, 2011

[2] J. Neubauer and E. Wood, "The impact of range anxiety and home, workplace, and public charging infrastructure on simulated battery electric vehicle lifetime utility," J. Power Sources, vol. 257, pp. 12–20, 2014.

[3] A. Seaman, T.S. Dao, and J. McPhee, "A survey of mathematics-based equivalent-circuit and electrochemical battery models for hybrid and electric vehicle simulation," J. Power Sources, vol. 256, pp. 410–423, 2014.

[4] X. Lin, H.E. Perez, S. Mohan, J.B. Siegel, A.G. Stefanopoulou, Y. Ding, et al, "A lumped-parameter electro-thermal model for cylindrical batteries," J. Power Sources, vol. 257, pp. 1–11, 2014.

[5] B.Y. Liaw, G. Nagasubramanian, R.G. Jungst, and Doughty DH, "Modeling of lithium ion cells a simple equivalent circuit model approach," Solid. State. Ionics, vol. 175, pp. 835–839, 2004.

[6] M. Dubarry and B.Y. Liaw, Development of a universal modeling tool for rechargeable lithium batteries. J. Power Sources, vol. 174, pp. 856–860, 2007.

[7] L. Lu, X. HAN, J. LI, J. Hua, and M. Ouyang, "A review on the key issues for lithium-ion battery management in electric vehicles," J. Power Sources, vol. 226, pp. 272-288, 2013.

[8] X. Hu, S. Li, and H. Peng, "A comparative study of equivalent circuit models for Li-ion batteries," J. Power Sources, vol. 198, pp. 359– 367, 2012.

[9] M. Doyle, T.F. Fuller, and J. Newman, "Modeling of Galvanostatic Charge and Discharge of the Lithium/Polymer/Insertion Cell," J. Electrochem. Soc., vol. 140, pp. 1526–1533, 1993.

[10] K. Smith and C.Y. Wang, "Solid-state diffusion limitations on pulse operation of a lithium ion cell for hybrid electric vehicles," J. Power Sources, vol. 161, pp. 628–639, 2006.

[11] S. Santhanagopalan and R.E. White, "Online estimation of the state of charge of a lithium ion cell," J. Power Sources, vol. 161, pp. 1346–1355, 2006.

[12] E. Prada, D.D. Domenico, Y. Creff, J. Bernard, V. Sauvant-Moynot, and F. Huet, "Simplified Electrochemical and Thermal Model of LiFePO4-Graphite Li-Ion Batteries for Fast Charge Applications," J. Electrochem. Soc., vol. 159, pp. A1508–1519, 2012;159.

[13] V.R. Subramanian, J.A. Ritter, and R.E. White, "Approximate Solutions for Galvanostatic Discharge of Spherical Particles. I. Constant Diffusion Coefficient," J. Electrochem. Soc. vol. 148, pp. E444–449, 2001.

[14] "Battery Test Manual for Plug-In Hybrid Electric Vehicles," USA: Idaho National Laboratory, INL/EXT-07-12536, Dec. 2010

[15] J.H. Holland, Adaptation in Natural and Artificial Systems: An Introductory Analysis with Applications to Biology, Control, and Artificial Intelligence. Massachusetts, USA: The MIT Press, 1992.